

Complete NLO corrections to off-shell $t\bar{t}Z$ production at the LHC

Daniele Lombardi^{a,*}

^a*Universität Würzburg, Institut für Theoretische Physik und Astrophysik, 97074 Würzburg, Germany*

E-mail: daniele.lombardi@physik.uni-wuerzburg.de

We present NLO-accurate predictions for the production and decay of a top–antitop pair in association with a Z boson at the LHC, in the multi-lepton decay channel. The complete set of LO contributions and NLO corrections of EW and QCD origin is included. The calculation is based on full matrix elements, computed with all resonant and non-resonant contributions, complete spin correlations and interference effects. Integrated and differential cross-sections are presented for a realistic fiducial setup.

*The European Physical Society Conference on High Energy Physics (EPS-HEP2023)
21-25 August 2023
Hamburg, Germany*

*Speaker

1. Introduction

The increasing amount of data that will be provided by the upcoming full Run-3 dataset and the future high-luminosity stage of the Large Hadron Collider (LHC) will allow to measure rare processes with an unprecedented accuracy. Among these rare signatures, the top-quark-associated Z-boson production ($t\bar{t}Z$ in the following) has already received great attention from the LHC experimental community in the past. The interest for this process is not limited to the fact that its accurate measurement offers an additional test to further confirm or eventually disprove the standard model (SM). Indeed, the study of $t\bar{t}Z$ production can also improve our understanding of the top-quark couplings with the electroweak (EW) sector, and the modelling of the background for other LHC processes, like $t\bar{t}H$ production with a leptonically decaying Higgs boson.

This growing level of experimental precision should be matched by theoretical predictions. Unfortunately, improving predictions for $t\bar{t}Z$ production is an extremely hard task, due to the high-multiplicity of the final state and the intricate resonance structure. Next-to-leading order (NLO) QCD and EW corrections for this process have been computed in the past, also supplemented by analytic resummation or parton-shower matching, but mostly with an approximate treatment of the resonance particles. Nevertheless, a proper modelling of off-shell effects is known to be crucial for an accurate description of observables which are differential in the decay products of the resonances.

The first off-shell calculation at NLO QCD for $t\bar{t}Z$ in the four-charged-lepton decay channel has been obtained in Ref. [1]. In this contribution, we present results for the same process which go one step forward in accuracy by computing the complete set of full off-shell LO and NLO corrections.

2. Structure of the calculation

In Ref. [2] the full set of NLO EW and QCD corrections to the process

$$pp \rightarrow e^+ \nu_e \mu^- \bar{\nu}_\mu b \bar{b} \tau^+ \tau^- \quad (1)$$

has been obtained for the first time. The calculation has been performed with the in-house program MoCANLO, a multichannel Monte Carlo generator which relies on RECOLA [3, 4] for the computation of the tree-level SM matrix elements and on the COLLIER library [5] for the reduction and numerical evaluation of the one-loop integrals. The complex-mass scheme [6, 7] for all unstable particles is used throughout, and the dipole subtraction formalism [8, 9] is employed for the treatment of QCD and QED singularities of infrared and collinear origin. The initial-state collinear singularities are absorbed in the parton-distribution functions (PDFs) in the $\overline{\text{MS}}$ factorisation scheme.

Spin-correlation and off-shell effects are fully taken into account by including the complete set of resonant and non-resonant Feynman diagrams. Therefore, subleading contributions involving a Higgs boson are also considered. Additionally to the dominant light-quark and gluon mediated partonic processes, all photon-induced channels are evaluated, together with the bottom-induced ones, consistently with the choice of a five-flavour scheme. This is done for all the perturbative orders contributing to the process. As schematically displayed in Fig. 1, $t\bar{t}Z$ receives three LO contributions at $\mathcal{O}(\alpha_s^2 \alpha^6)$, $\mathcal{O}(\alpha_s \alpha^7)$ and $\mathcal{O}(\alpha^8)$, that we name LO₁, LO₂, and LO₃, respectively, and consequently four kinds of NLO corrections at $\mathcal{O}(\alpha_s^3 \alpha^6)$ (NLO₁), $\mathcal{O}(\alpha_s^2 \alpha^7)$ (NLO₂), $\mathcal{O}(\alpha_s \alpha^8)$ (NLO₃), and $\mathcal{O}(\alpha^9)$ (NLO₄). In our full prediction, the different orders are combined in an additive way.

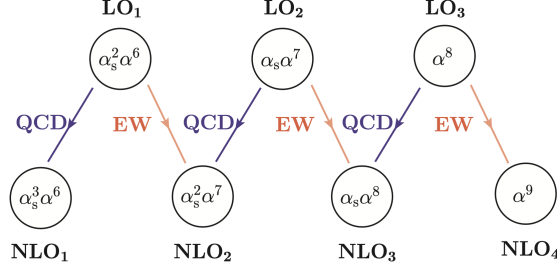


Figure 1: Perturbative orders contributing at LO and NLO for the process in Eq. (1).

3. Numerical results

We present results for the LHC at a centre-of-mass energy of 13 TeV for the reaction in Eq. (1) in the fiducial region described in Ref. [2]. QCD partons with pseudorapidity $|\eta| < 5$ are clustered into jets using the anti- k_t algorithm [10] with resolution radius $R = 0.4$. To guarantee the IR safety of the result when three bottom quarks occur in the final state, we recombine a b jet and a light jet into a b jet, and two b jets into a light jet. At least two b jets are required in the final state, fulfilling $p_{T,b} > 25$ GeV, $|\eta_b| < 2.5$, and $\Delta R_{bb} > 0.4$. Charged leptons are dressed with the anti- k_t clustering algorithm with $R = 0.1$, and have to satisfy $p_{T,\ell_i} > 20$ GeV, $|\eta_{\ell_i}| < 2.5$, and $\Delta R_{\ell_i \ell_j} > 0.4$, where $\ell_i \in \{e^+, \mu^-, \tau^+, \tau^-\}$. Additionally, a cut on the missing transverse momentum arising from the undetected neutrinos $p_{T,\text{miss}} > 40$ GeV is imposed. The factorization and renormalization scales are chosen according to

$$\mu_0^{(d)} = \frac{1}{2} (M_{T,t} M_{T,\bar{t}})^{1/2} = \frac{1}{2} \left(\sqrt{m_t^2 + p_{T,t}^2} \sqrt{m_t^2 + p_{T,\bar{t}}^2} \right)^{1/2}, \quad (2)$$

where $m_t = 173.0$ GeV and the top and antitop transverse momenta are reconstructed from their decay products based on the Monte Carlo truth. Using $\mu_0^{(d)}$ as central scale, uncertainties in the results are estimated with the standard 7-point scale variation.

3.1 Fiducial cross-sections

In Table 1 results for integrated cross-sections are presented at different perturbative accuracies. In the second column, the integrated cross-section σ_{nob} accounts for all partonic channels, except the ones involving at least one bottom quark in the initial state, whose contribution σ_b is separately reported in the fourth column. The full prediction $\sigma = \sigma_{\text{nob}} + \sigma_b$, including all partonic channels, is shown in the sixth column.

The dominant correction is clearly the NLO₁ one, which modifies the LO₁ cross-section by -10% and largely reduces the size of scale uncertainties. Subleading contributions have a minor impact on the full prediction: the sum of the LO₂ and LO₃ results amounts to $+1\%$ of the LO₁, while the NLO₂ and NLO₃ corrections all together affect the LO₁ result at the sub-percent level. Bottom-induced channels play a minor role at the inclusive level, with an impact of roughly $+1\%$ on the full prediction once their contribution is accounted for both at LO and NLO. For all channels, the NLO₄ corrections, whose full off-shell calculation turns out to be a formidable task, are entirely negligible.

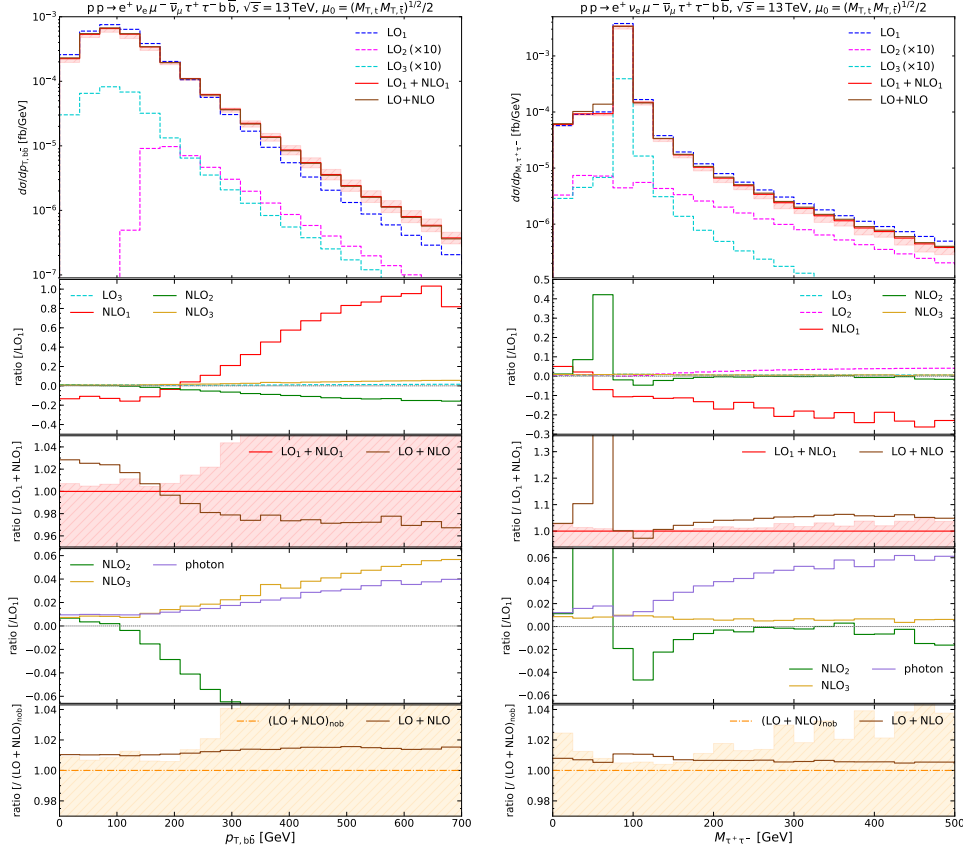
perturbative order	σ_{nob} [ab]	$\frac{\sigma_{\text{nob}}}{\sigma_{\text{nob}, \text{LO}_1}}$	σ_{b} [ab]	$\frac{\sigma_{\text{b}}}{\sigma_{\text{nob}, \text{LO}_1}}$	σ [ab]	$\frac{\sigma}{\sigma_{\text{LO}_1}}$
LO ₁	107.246(5) ^{+35.0%} _{-24.0%}	1.0000	0.31378(9)	+0.0029	107.560(5) ^{+34.9%} _{-23.9%}	1.0000
LO ₂	0.7522(2) ^{+11.1%} _{-9.0%}	+0.0070	-0.6305(2)	-0.0059	0.1217(3)	+0.0011
LO ₃	0.2862(1) ^{+3.4%} _{-3.4%}	+0.0027	0.7879(2)	+0.0073	1.0742(3) ^{+12.1%} _{-14.9%}	+0.0100
NLO ₁	-11.4(1)	-0.1072	0.518(3)	+0.0048	-10.9(1)	-0.1016
NLO ₂	-0.89(1)	-0.0083	0.109(3)	+0.0010	-0.78(1)	-0.0072
NLO ₃	1.126(4)	+0.0105	-0.089(4)	-0.0008	1.037(6)	+0.0096
NLO ₄	-0.0340(9)	-0.0003	-0.0180(9)	-0.0002	-0.052(1)	-0.0005
LO ₁ +NLO ₁	95.8(1) ^{+0.4%} _{-11.2%}	+0.8933	0.832(3)	+0.0078	96.6(1) ^{+0.4%} _{-10.7%}	+0.8984
LO	108.285(5) ^{+34.7%} _{-23.8%}	+1.0097	0.4713(3)	+0.0044	108.756(5) ^{+34.5%} _{-23.7%}	+1.0111
LO+NLO	97.0(1) ^{+0.5%} _{-11.2%}	+0.9052	0.991(6)	+0.0092	98.0(1) ^{+0.4%} _{-10.6%}	+0.9114

Table 1: LO cross-sections and NLO corrections (in ab) in the fiducial setup. In the second column all partonic channels are included in σ_{nob} except the ones having at least one bottom quark in the initial state, while σ_{b} includes all these channels. The sum of the two (σ) is shown in the sixth column. Ratios with respect to the cross-section σ_{nob} at LO₁ accuracy are reported in the third and fifth column. In the seventh column ratios are shown with respect to the full LO₁ cross-section including the bottom channels, as well. Integration errors are given in parentheses and percentage 7-point scale variations as super- and sub-scripts.

3.2 Differential cross-sections

In Fig. 2 we present results for two exemplary distributions. In a main panel the three LO contributions are presented with dashed lines, namely the LO₁ (blue curve), the LO₂ (magenta curve) and LO₃ (turquoise curve). The last two contributions are shown after scaling them up by a factor of 10. In the same panel, the genuine NLO QCD result, i.e LO₁ + NLO₁, is shown in red, together with the full NLO prediction LO+NLO, shown in brown. In a first ratio panel we present the three NLO corrections, namely NLO₁ (in red), NLO₂ (in green), and NLO₃ (in goldenrod), normalised to the LO₁ result, while in a second panel the LO₁ + NLO₁ result and the complete LO+NLO prediction (both normalised with respect to the former) are compared. A third ratio panel shows the importance of the photon-induced contribution (accounting for all channels with at least one photon as an initial-state parton) with a purple curve, in comparison with the NLO₂ and NLO₃ corrections. All curves are normalised here to the LO₁ result. Finally, a last panel illustrates the impact of bottom-induced contributions. The full LO+NLO prediction is reported together with the (LO + NLO)_{nob} result (dash-dotted orange curve), where all channels with at least one initial-state bottom have been excluded: the latter prediction is also used for normalisation.

The distribution in the transverse momentum of the $b\bar{b}$ pair in Fig. 2(a) is particularly sensitive to QCD corrections, which in the tails of the distribution increase up to +100%, as a result of enhanced $t\bar{t}j$ topologies where the emission of a soft and/or collinear Z boson leads to a giant QCD K -factor [11]. The LO₃ curve in the main frame mimics the shape of the LO₁ result, while the LO₂ term is peaked at higher values, as a consequence of a destructive interference of the bottom-



(a) Transverse momentum of the bottom-jet pair

(b) Invariant mass of the $\tau^+\tau^-$ pair

Figure 2: Distributions in the transverse momentum of the bottom-jet pair (left) and in the invariant mass of the $\tau^+\tau^-$ pair (right). The different NLO corrections for the observables are compared separately (first ratio panels) and at the level of the full prediction (second ratio panel). The size of photon-induced channels and bottom contributions are presented in the third and fourth ratio panels, respectively.

and γg -induced channels for low $p_{T,b\bar{b}}$ values in the fiducial setup considered here. The subleading NLO corrections also show a non-trivial interplay. The NLO_2 term provides large and negative contributions in the tails, due to the effect of EW Sudakov logarithms [12], which reach about -15% at $p_{T,b\bar{b}} = 700$ GeV. A positive $+5\%$ correction in the same region arises instead from the NLO_3 contribution. On the other hand, the impact of the bottom channels on this observable, whose definition requires two b jets, is moderate, namely $+1\%$ in the bulk of the distribution and $+1.5\%$ in its tail.

The distribution in the invariant mass of the $\tau^+\tau^-$ pair in Fig. 2(b) shows the usual peak at the Z-boson mass for LO_1 and LO_3 , but a slight dip for LO_2 , whose curve presents hard tails amounting to a $+4\%$ correction to LO_1 . This behaviour is entirely driven by the γg channels, and specifically by the rapid growth of photon PDF in that region. Among NLO contributions, the NLO_1 one dominates in the far off-shell region with a -20% correction of the LO_1 , while photon radiative effects included in the NLO_2 term provide a $+40\%$ correction right below the peak. The NLO_3 contribution is instead quite small and essentially flat, similarly to the effect of bottom-induced channels on the full NLO prediction.

4. Conclusions

We have presented the first complete calculation of the off-shell production of a top–antitop pair in association with a Z boson for 13 TeV proton–proton collisions, computing the entire tower of LO contributions and NLO corrections. We have shown that subleading LO and NLO contributions are essential for a precise description of many observables, which present not just a change in normalisation, but also shape distortions once those contributions are properly included.

Acknowledgements

This contribution is based upon work supported by the German Federal Ministry for Education and Research (BMBF) under contract no. 05H21WWCAA.

References

- [1] G. Bevilacqua, H. B. Hartanto, M. Kraus, J. Nasufi and M. Worek, *JHEP* **08** (2022), 060 doi:10.1007/JHEP08(2022)060 [arXiv:2203.15688 [hep-ph]].
- [2] A. Denner, D. Lombardi and G. Pelliccioli, *JHEP* **09** (2023), 072 doi:10.1007/JHEP09(2023)072 [arXiv:2306.13535 [hep-ph]].
- [3] S. Actis, A. Denner, L. Hofer, A. Scharf and S. Uccirati, *JHEP* **04** (2013), 037 doi:10.1007/JHEP04(2013)037 [arXiv:1211.6316 [hep-ph]].
- [4] S. Actis, A. Denner, L. Hofer, J. N. Lang, A. Scharf and S. Uccirati, *Comput. Phys. Commun.* **214** (2017), 140-173 doi:10.1016/j.cpc.2017.01.004 [arXiv:1605.01090 [hep-ph]].
- [5] A. Denner, S. Dittmaier and L. Hofer, *Comput. Phys. Commun.* **212** (2017), 220-238 doi:10.1016/j.cpc.2016.10.013 [arXiv:1604.06792 [hep-ph]].
- [6] A. Denner and S. Dittmaier, *Nucl. Phys. B Proc. Suppl.* **160** (2006), 22-26 doi:10.1016/j.nuclphysbps.2006.09.025 [arXiv:hep-ph/0605312 [hep-ph]].
- [7] A. Denner and S. Dittmaier, *Phys. Rept.* **864** (2020), 1-163 doi:10.1016/j.physrep.2020.04.001 [arXiv:1912.06823 [hep-ph]].
- [8] S. Catani and M. H. Seymour, *Nucl. Phys. B* **485** (1997), 291-419 [erratum: *Nucl. Phys. B* **510** (1998), 503-504] doi:10.1016/S0550-3213(96)00589-5 [arXiv:hep-ph/9605323 [hep-ph]].
- [9] S. Dittmaier, A. Kabelschacht and T. Kasprzik, *Nucl. Phys. B* **800** (2008), 146-189 doi:10.1016/j.nuclphysb.2008.03.010 [arXiv:0802.1405 [hep-ph]].
- [10] M. Cacciari, G. P. Salam and G. Soyez, *JHEP* **04** (2008), 063 doi:10.1088/1126-6708/2008/04/063 [arXiv:0802.1189 [hep-ph]].
- [11] M. Rubin, G. P. Salam and S. Sapeta, *JHEP* **09** (2010), 084 doi:10.1007/JHEP09(2010)084 [arXiv:1006.2144 [hep-ph]].
- [12] A. Denner and S. Pozzorini, *Eur. Phys. J. C* **18** (2001), 461-480 doi:10.1007/s100520100551 [arXiv:hep-ph/0010201 [hep-ph]].